PRELIMINARY ANALYSIS OF BRAIN PERFUSION OBTAINED WITH ARTERIAL SPIN LABELING METHOD (ASL) USED TO EVALUATE THE EFFECTS OF TYPE 2 DIABETES IN MORBIDLY OBESE PATIENTS

Anna KĘDZIORA[1], Michał KACPRZAK[2], Ewa PIĄTKOWSKA-JANKO[1]

1 Institute of Radioelectronics and Multimedia Technology, Warsaw University of Technology, 15/19 Nowowiejska St, 00-665 Warsaw, Poland

2 Nalecz Institute of Biocybernetics and Biomedical Engineering, Polish Academy of Sciences, Ks. Trojdena str 4, 02-109 Warsaw, Poland

Author's address: E. Piątkowska-Janko, Institute of Radioelectronics and Multimedia Technology, Warsaw University of Technology, 15/19 Nowowiejska St, 00-665 Warsaw, Poland, e-mail: ewa.piatkowska@pw.edu.pl

Introduction: Earlier studies demonstrated that obesity was associated with lower cerebral perfusion in obese participants, as compared to participants at normal weight, especially in frontal grey matter regions. On the other hand, type 2 diabetes is a common co-morbid condition among obese patients, and it is associated per se with brain structural and metabolic abnormalities that are related to lower cerebral blood flow (CBF). Unfortunately, only two studies evaluated the effects on co-morbid T2D on CBF, one of them in adolescent population. Therefore, the aim of this study was to establish a pipeline process to quantify CBF images that were obtained in an independent project evaluating brain abnormalities associated with morbid obesity and their resolution with intragastric balloon – an invasive method to reduce weight. Furthermore, we compared CBF between obese patients with and without type 2 diabetes, as well as controls at normal weight.

Methods: A processing pipeline utilizing SPM12 toolbox and digital maps (AAL, Brodmann) was established to automatically pre-process scans and toolbox REX was used to prepare data for statistical analysis. We used it to analyze data for six morbidly obese patients with type 2 diabetes T2D (O-T2D) (average age = 48.5 ± 7.9, average body weight = 125.0 ± 29.8 kg, average BMI = 42.0 ± 9.4), eight morbidly obese patients without T2D (O-NT2D) (average age = 39.1 ± 16.1, average body weight = 138.2 ± 14.9 kg, average BMI = 50.2 ± 6.5) and eight healthy controls with normal weight (CON) (average age = 43.5 ± 11.5, average body weight = 67.4 ± 14.6 kg, average BMI = 23.4 ± 3.5). All studies were performed at the CNS Lab MRI Centre, NIBBE.

Results: These preliminary analyses demonstrated lower cerebral blood flow in frontal cortex in obese patients with T2D, as compared to obese patients without T2D and controls.

Conclusion: A pipeline to numerically process ASL-CBF data was created and used to analyse the small dataset. The analyses indicated that not morbid obesity per se, but morbid obesity combined with co-morbid type 2 diabetes is associated with widespread reductions in cerebral perfusion. The results are in line with other studies that were limited to subjects with lower stages of overweight and obesity. We believe that this methodology may be applied to study changes in brain perfusion evoked by simulated hypergravity with Lower-Body Negative Pressure (LBNP) device placed within a magnetic resonance scanner or perfusion changes induced by hypoxia.

Keywords: arterial spin labelling, cerebral blood flow, pre-processing, brain atlas, statistical analysis, Matlab, SPM12

INTRODUCTION

The brain is the most complex and sensitive organ of the human body. In case of abnormalities in its functioning it is important to quickly determine where the abnormalities come from. One of the methods of medical imaging used in clinical applications is nuclear magnetic resonance imaging (MRI). One of the parameters determined during MRI examination is blood perfusion, i.e. the process of blood flow through the brain. The methods used so far have been based on the use of a contrast agent. The disadvantage of such methods is their invasiveness and low accuracy of obtained results. In 1992, an article was published, which proposed a breakthrough method of determining the cerebral blood flow – Arterial Spin Labelling (ASL) [28]. This method is based on marking the spins of blood protons flowing at the neck level. The unrivalled advantage of this method is its complete non-invasiveness - the only marker used is the one found in blood. Other advantages are the speed of the examination, no contraindications due to health condition and no need for convalescence.

Neuroimaging studies reported morphological changes in the brains of obese individuals [26], whereas magnetic resonance spectroscopic studies showed lower concentrations of N-acetylo-aspartate (NAA) that is a marker of neuronal integrity [10,11] suggesting slowed down neuronal metabolism. Other studies demonstrated lower glucose metabolism [24] and lower cerebral blood flow (perfusion) [2,4,17,19,27] in multiple brain regions in overweight and obese individuals without T2D that could be revered with physical activity [17]. Magnetic resonance spectroscopic study of diabetic patients demonstrated similar pattern of lower NAA concentrations and increased myo-in-

ositol concentrations throughout the brain, suggesting inflammatory state [21]. However, among morbidly obese patients with type 2 diabetes only elevated myo-inositol was detected; it normalized within six months after bariatric intervention [12]. Only two studies evaluated the effects of comorbid T2D in obesity on cerebral blood flow. One of them demonstrated lower CBF in multiple brain regions in a group of twenty obese adolescents as compared to their age and BMI matched counterparts without type 2 diabetes mellitus [20], whereas the other demonstrated reduced normalized CBF only in insula of 43 middle-aged obese participants with T2D, as compared to 20 age-matched controls using SPECT imaging [16].

Here, we established a pipeline process to quantify CBF images in order to evaluate the effects of co-morbid type 2 diabetes mellitus on cerebral blood flow in morbidly obese patients.

MATERIALS AND METHODS

Participants

The analyses were performed on data acquired in an independent project evaluating functional and structural brain changes accompanying intragastric balloon induced weight loss [8,9,12-14]. The control group (CON) consisted of eight healthy individuals whose average age was 43.50 ± 11.46 years, average body weight was 67.4 ± 14.63 kg and average BMI 23.36 ± 3.50; the obese group without diabetes (O-NT2D) consisted of eight persons with an average age of 39.13 ± 16.10 years, an average body weight of 138.19 ± 14.87 kg and an average BMI of 50.19 ± 6.49, while the obese group with diabetes (O-T2D) consisted of six persons with an average age of 48.50 ± 7.87

years, an average body weight of 125.02 ± 29.77 kg and an average BMI of 42.00 ± 9.40. The patients were treated at the Military Institute of Aviation Medicine in Warsaw. All participants gave written informed consent to all procedures prior to the study. All procedures had been approved by the Institutional Review Board of the Military Institute of Aviation Medicine, Warsaw, Poland (decision no 05/2012) and have been performed in accordance with the ethical standards as laid down in the 1964 Declaration of Helsinki and its later amendments or comparable ethical standards.

Arterial Spin Labelling - Methodology

The method of marking arterial blood spins ASL is based on the magnetic properties of flowing blood and consists in the inversion of hydrogen proton spins found in arterial blood. In the ASL sequence it performs. The data is acquired in two data volumes - control without inversion pulse and with marked spins. The difference between them is an image of cerebral perfusion, a base to calculate maps CBF blood flow. In general, there are three types of spins marking: continuous, pseudo-continuous and intermittent. ASL uses hydrogen molecules found in arterial blood as an endogenous and diffusion-transferable marker, reversing the magnetization of blood spins using radiofrequency (RF) energy pulses. In the beginning, the control image is acquired, the spins are then in balance. Then the magnetization of the blood spins is reversed by 180°, using one of the marking methods. After a delay time, allowing the blood to reach the brain tissue, another image acquisition is performed, which contains a signal from the marked blood. The difference between the image with marked pins and the control image provides information about the amount of blood that has flowed into the brain during the time from marking to data acquisition and is an image of the cerebral flow of CBF blood [3]. Below

are the drawings (fig 1,2) showing the principle of ASL.

Figure 1 shows the marked area in which the control image is acquired. In the area marked with the number 2, the blood spins are inverted by 180°. Then, after the Post-Labeling Delay (PLD) time, selected according to the patient, needed for the passage of the marked spins from the area marked with number 2 to the area number 1, the image containing the marked spins is acquired.

Figure 2 shows the step of subtracting the control image from the image with marked pins on a pixel-by-pixel basis. This operation returns the initial image, containing the difference between the two images, giving information about the amount of blood that has flowed to the brain in a given period of time.

There are three methods of marking spins: 1) pulsed ASL (PASL), 2) continuous ASL (CASL), and 3) pseudo-continuous ASL (PCASL).
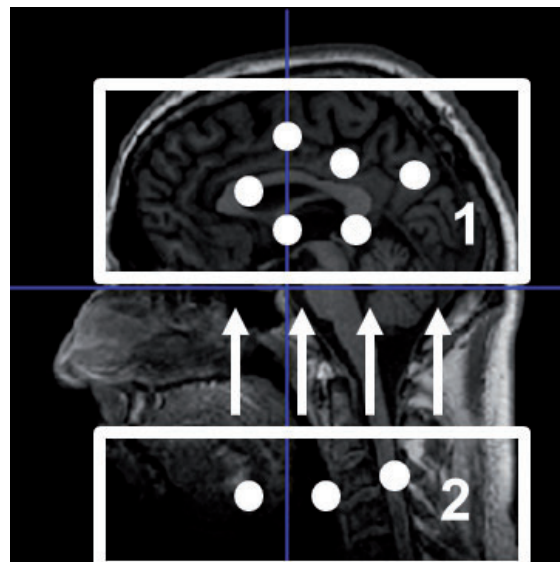

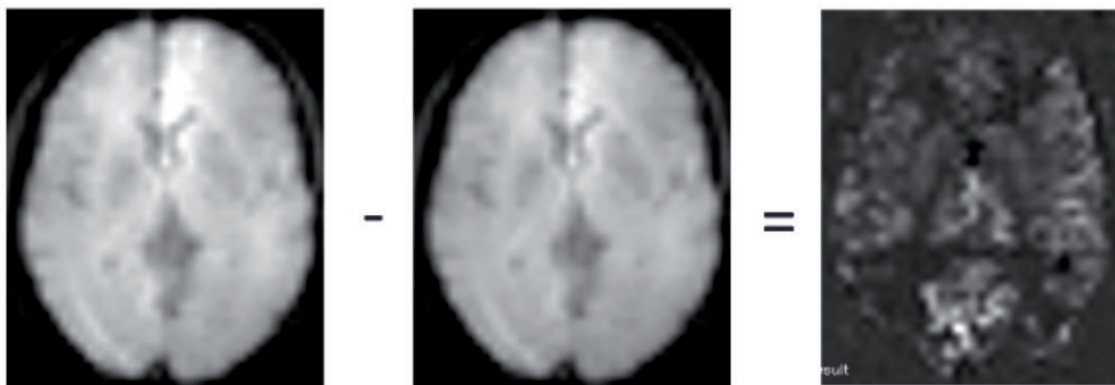Fig. 1.   Spin marking and image acquisition [7].

Fig. 2.   Determination of the blood flow map by subtracting images from each other [7].

In the intermittent method, marking takes place in a given volume using a short pulse or a specific number of pulses, whose total duration is usually 10 ÷ 20 ms (Fig 3). The width of the marking area is usually 15 ÷ 20 cm. In the PASL method a high signal-to-noise ratio is achieved [3].

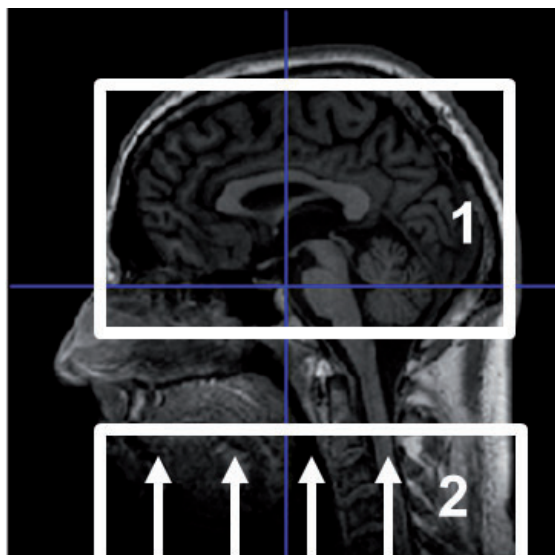Fig. 3.   PASL marking of spins [7].

In the continuous method, the marking of the spins takes place in a thin plane at neck level. Spins are inverted by means of a continuous pulse of radio frequency energy, lasting 2 ÷ 4 seconds (Fig 4). The volume of marked blood is proportional to the duration of the energy pulse, and the efficiency of marking depends on the speed of blood flow. The advantage of this method is high contrast, but the signal coming from the blood is weak [3].
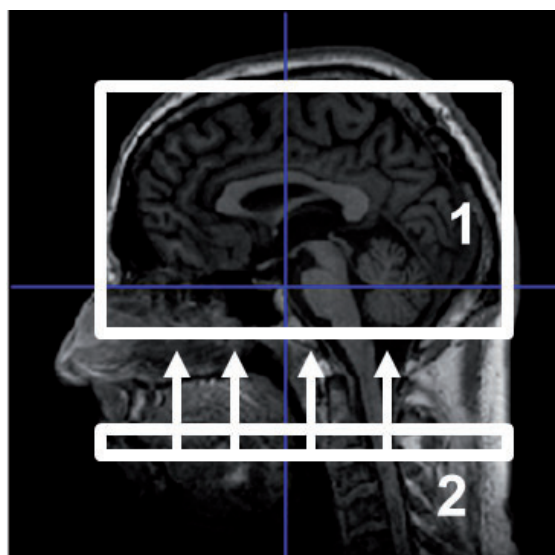

Fig. 4.   CASL marking of spins [7].

Both the PASL and CASL methods require that the tissue signal obtained during the acquisition of the control image and with the marked pins is the same. This is due to the fact that the blood signal is weak. The occurrence of differences may lead to distortions in the resultant image.

Therefore, the PCASL method is a modification of the CASL method that uses some elements of the PASL method. In the pseudo-continuous method, marking is done by applying a thousand or more radio frequency pulses. Their total duration is about 1.5 ÷ 2 s. The advantage of this method is high efficiency of marking and reduced effect of magnetization transfer to the obtained signal [3].

PLD time, this is the time interval from the end of the RF pulse to the image acquisition and is needed for the blood to flow from the neck area to the imaging area. If the inversion time is too short, the blood will not be able to reach the data acquisition area, similarly for too long, signal loss will occur due to longitudinal blood relaxation. PLD time, depends on age, gender and tissue health and can vary by several hundred milliseconds for individual patients. It is selected individually by the technician immediately before the examination [3].

Image data acquisition

All participants underwent structural imaging in a 3T GE Discovery 750w with 70cm wide bore, (located in CNS Lab MRI Centre, NIBBE) using a body transmit coil for excitation and an eight-channel receive coil. The T1-weighted structural scan was obtained with the following parameters (TR/TE/TI=6.5/2.1/400ms, 1x1x1mm3).

CBF measurement used pseudo-continuous arterial spin labeling (pCASL; utilizing 3D Spiral Fast Spin Echo sequences, TR/TE/TI = 4640/10.704/2025 ms, 1.875×1.875 mm2 in-plane resolution, 4 mm slice thickness, no gap, covering the entire brain, post-labelling delay 2025ms, 50 averages, duration 4 min 22 sec).

The CBF maps are automatically determined after the 3DASL sequence. (described in chapter 3.2) The size of the CBF image matrix was 128 x 128 x 36 voxels and the size of the voxel was 1.88 x 1.88 x 4 mm.

CBF was calculated according to recommendations [3] by the MRI scanner in milliliters of blood per 100g of brain tissue per minute.

Simplified course of the sequence is shown in Figure 5. At the beginning, an inversion impulse is sent, the purpose of which is to suppress the background, then the marking of blood spins with
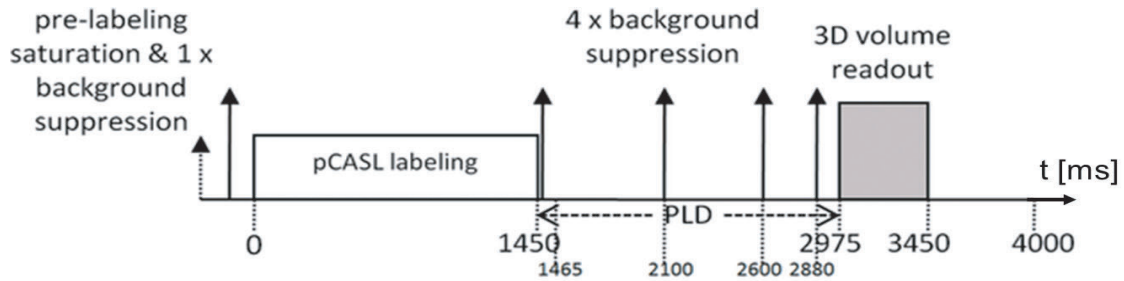
Fig. 5.   3D ASL sequence diagram (GE sequence timing diagram based on [18]).

the PCASL method is carried out by means of a sequence of impulses. After switching off the impulses and waiting for PLD time, 3D data acquisition takes place. In the interval between marking and acquisition, another four inversion pulses are sent, which are responsible for background suppression. The other important parameters of the 3DASL sequence are: duration of the inversion: 1450 ms, duration of the inversion pulse: 0.5 ms, recording of space k: in a spiral manner, through 8 spirals with 512 measuring points each, - number of layers: 36, background suppression: 1 pulse before marking and 4 during the PLD [1]. The map of cerebral CBF blood flow is calculated automatically in the GE MRI console. The values contained in the image are expressed in units of CBF, that is. A formula is used to calculate the CBF map:

$$CBF = \frac{6000k\left(1 - e^{-\frac{t_{sat}(s)}{T_{1t}(s)}}\right)e^{\frac{PLD(s)}{T_{1a}(s)}}}{2T_{1a}(s)\left(1 - e^{-\frac{\tau(s)}{T_{1a}(s)}}\right)\varepsilon AV_{\Delta M}}\left(\frac{\Delta M}{\alpha_{\Delta M}PD}\right)$$

where:
  k - scaling factor (default 0.9),
  e - the basis of natural logarithm,
  tsat - saturation time (default 2.0 s),
  T1t - relaxation time of the grey matter (default 1.2 s),
  PLD - interval from the end of the RF pulse to data acquisition,
  T1a - longitudinal blood relaxation time (default 1.6 s),
  τ- duration of RF pulses (default 1450 ms),
  ε - a combination of inversion pulse efficiency and background suppression (default 0.6),
  AVΔM - number of measurement averages,
  ΔM - the difference between the control image and the marked image,
  αΔM - control image scaling factor (default 32),
  PD - value of the control measurement signal [18].

Data preprocessing

Data analysis was performed using SPM12 (Statistical Parametric Mapping) toolbox developed in the Functional Imaging Laboratory at London University College by a team led by Professor Karl Friston. It is a free and publicly available toolbox that works with MATLAB [15]. The toolbox is designed to process MRI data, display and pre-process scans, and for statistical analysis.

Analysis of image data must be preceded by a series of spatial transformations, which are called pre-processing. These transformations are intended to reduce unwanted differences between voxels from different scans, which may be caused by movement during the study or by a shape difference between the scan series. Pre-processing is necessary both for the analysis of scans from a group of subjects as well as from a single patient. Analysis based on the comparison of the voxels requires that they come from the same part of the brain in all scans. Failure to meet this requirement will result in critical errors and differences in results. The pre-processing steps are listed in Figure 6. After each step, a visual assessment of the correctness of the transformation was carried out, so as to possibly correct or eliminate incorrectly processed data.
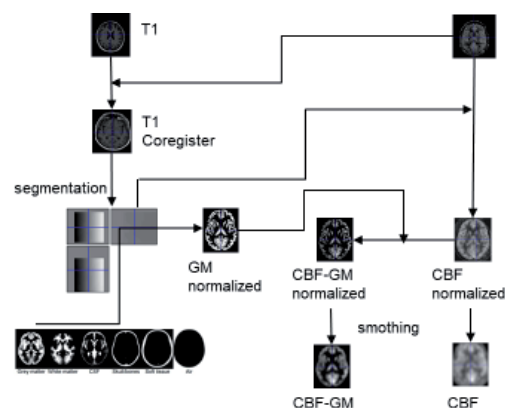

Fig. 6.   Diagram showing the next steps of data processing.

Briefly, T1 and CBF images of each individual subject were coregistered, segmented, normalized to an MNI template with affine registration followed by nonlinear transformation. Using the ImCalc function (SPM12), the CBF image was multiplied with grey matter segmented image,
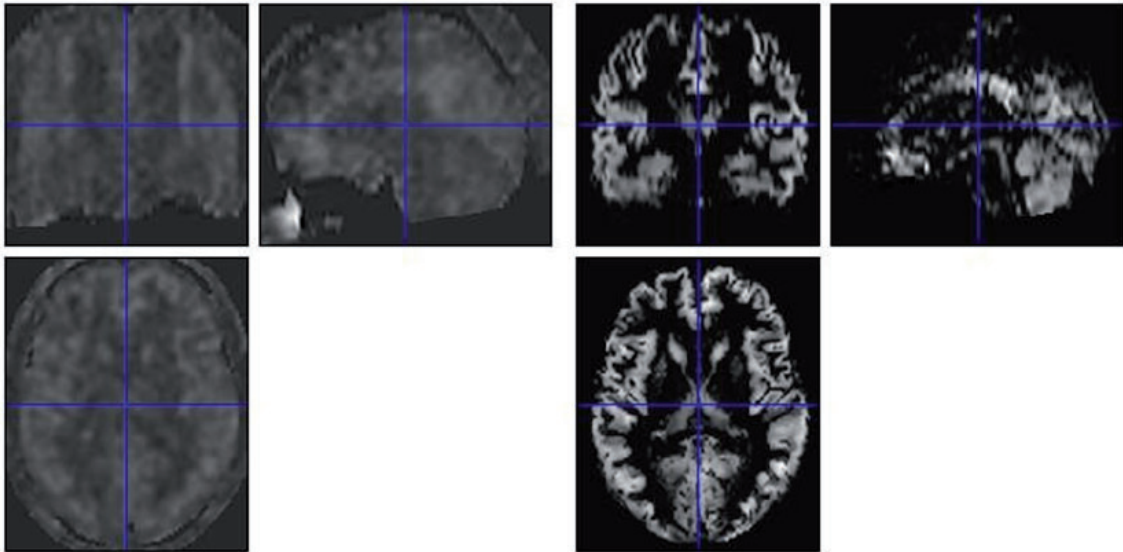
Fig. 7.   Example images of CBF and CBF-GM used for statistical analysis.

obtained a CBF grey image, representing the cerebral blood flow in the grey matter (CBF-GM).

Both CBF and CBF-GM images were smoothed with a Gaussian kernel of 16mm. For each subject, the CBF scans and the T1 scans after correction have been visually assessed for correctness of their matching. As a result of the assessment, two scans from the control group, two scans from the obese group without diabetes and one scan from the obese group with diabetes were rejected. The reasons for rejection of these scans were: artefacts occurring in specific areas of the brain, the cut-off part of the brain and inaccuracy of the algorithm for matching data to each other. Finally, the scans of six subjects in the control group, six subjects in the obese group without diabetes and five subjects in the obese group with diabetes were further processed.

Brain Atlases

The brain atlas is an anatomical representation of the brain, created by using scans of a dozen or so people. The atlas is created by statistically averaging the location and size of the voxels of all scans. Such an atlas consists of numbered structures, which represent anatomical structures or functionality. They are used, among others, in statistical research and as support during operations. [9] In this paper, the AAL and Brodmann atlases were used for image analysis.

The AAL Atlas is an anatomical representation of spatially standardized high resolution T1 images from MNI. The atlas is the result of automatic marking of 116 anatomical structures of 45 standardized individual scans of high-resolution T1 images from the Institute of Montreal (MNI) [23].

The German anatomist Korbinian Brodmann defined 52 areas later named after him at the beginning of the 20th century, which were based on the cytoarchitectonic organization of neurons in the cerebral cortex. Today's atlas is slightly different from the original one and consists of individual fields: The Brodmann atlas used in this work consists of 41 structures [5].

Figure 7 shows example images of CBF and CBF-GM, on which statistical analysis was then performed.

Statistical analysis of data

The statistical analysis of the CBF and CBF-GM images was performed both on ROI-based analysis, and whole brain voxel –base analysis.

The REX Toolkit, part of the large Toolkit (CONN) [25] was used for ROI-based analysis. The mean values for the regions from the AAL and Brodmann atlases were determined on the basis of the whole brain (CBF) and gray matter (CBF-GM) images.

RESULTS ANALYSIS AND CONCLUSIONS

The number of control group and obese people without diabetes was six each, while obese people with diabetes were five each.

To illustrate the differences for each group, means and standard deviations of whole brain were calculated, therefrom to give an overview of the study. The data are summarized in Table 1.

The results between the different atlases within the same image are similar, and the differences are due to different sets of structures under consideration, dictated by different results of the t-test. There is a clear difference between cerebral

Technical Note

Tab. 1. Comparison of group results for whole brain different atlases and images; CON - control group, O-NT2D - obese without diabetes, O-T2D - obese with diabetes.

	Image/Atlas	mean ml/100 g/min			Standard deviation ml/100 g/min		
		O-NT2D	O-T2D	CON	O-NT2D	O-T2D	CON
CBF	AAL	54.07	36.226	41.71	12.51	5.24	7.43
	Brodmanna	53.78	36.04	-	11.87	4.92	-
CBF-GM	AAL	28.41	16.95	24.34	7.88	3.56	7.10
	Brodmanna	27.84	16.44	-	7.51	3.06	-

Tab. 2. Difference between group CON and O-T2D for ROI analysis – CBF map and AAL atlas.

ROI from AAL atlas	p	T-test	Mean CON	SD CON	Mean O-T2D	SD O-T2D
Postcentral_L	0.033	-2.470	39.916	6.912	52.659	10.580
Precentral_L	0.040	-2.360	41.365	7.499	54.681	11.609
SupraMarginal_L	0.047	-2.266	43.838	7.867	56.731	11.502

Tab. 3. Difference between group O-NT2D and O-T2D for ROI analysis – CBF map and AAL atlas.

ROI from AAL atlas	p	T-test	Mean O-NT2D	SD O-NT2D	Mean O-T2D	SD O-T2D
Frontal_Mid_R	0.001	4.851	54.065	9.195	32.733	3.598
Temporal_Pole_Mid_L	0.001	4.551	46.472	5.366	33.273	3.952
Frontal_Sup_L	0.002	4.464	50.245	8.990	31.343	3.002
Frontal_Sup_R	0.002	4.332	50.043	9.489	30.891	2.720
Frontal_Mid_L	0.002	4.305	56.982	11.046	34.759	3.320
Frontal_Mid_Orb_L	0.002	4.311	53.313	8.552	35.677	3.353
Precentral_L	0.004	3.798	54.681	11.609	33.860	3.990
Frontal_Inf_Tri_L	0.004	3.921	58.538	10.954	38.097	4.094
Frontal_Inf_Tri_R	0.004	3.922	52.077	8.292	35.704	4.584
Frontal_Inf_Orb_L	0.004	3.837	56.080	9.824	37.816	4.290
Supp_Motor_Area_L	0.004	3.844	56.730	11.972	35.330	3.317

Tab. 4. Difference between group CON and O-T2D for ROI analysis – CBF-GM and AAL atlas.

ROI from AAL atlas	p	T-test	Mean CON	SD CON	Mean O T2D	SD O-T2D
Occipital_Mid_R	0.028	2.620	24.188	7.624	14.472	3.427
Angular_L	0.035	2.483	24.490	6.583	16.478	3.117

Tab. 5. Difference between group O-NT2D and O-T2D for ROI analysis – CBF-GM and AAL atlas.

ROI from AAL atlas	p	T-test	Mean O NT2D	SD O-NT2D	Mean O-T2D	SD O-T2D
Temporal_Pole_Mid_L	0.001	4.886	21.657	3.301	13.425	1.951
Precentral_L	0.003	4.064	24.865	6.538	12.639	1.453
Frontal_Mid_R	0.003	4.034	25.755	6.824	12.984	1.811
Supp_Motor_Area_L	0.003	4.049	28.037	7.281	14.341	1.987
Postcentral_L	0.003	4.084	22.760	5.958	11.529	1.428
Temporal_Pole_Sup_L	0.003	4.091	26.079	5.558	15.037	2.466
Frontal_Sup_L	0.004	3.832	22.654	5.807	12.161	1.967
Frontal_Sup_R	0.004	3.896	22.755	6.023	11.861	1.625
Frontal_Mid_Orb_L	0.004	3.794	26.006	6.180	14.735	2.535
Frontal_Inf_Orb_L	0.004	3.834	29.537	6.514	17.460	2.802
Parietal_Inf_L	0.004	3.789	27.361	7.751	13.431	2.798
SupraMarginal_L	0.004	3.900	30.358	7.518	16.169	3.252
Caudate_L	0.004	3.839	17.533	3.642	10.681	1.723
Frontal_Mid_L	0.005	3.748	27.111	7.307	14.012	2.863
Frontal_Inf_Tri_L	0.005	3.662	30.187	7.822	16.352	3.336
Angular_L	0.005	3.710	30.972	8.195	16.478	3.117
Paracentral_Lobule_L	0.005	3.678	20.940	6.216	10.229	1.934

Tab. 6.   Difference between group O-NT2D and O-T2D for ROI analysis – CBF and Brodmann atlas.

ROI from atlas	p	T-test	SD	Mean O-NT2D	SD O-NT2D	Mean O-T2D	SD O-T2D
Brodmann_area_39	0.001	4.504	7.550	55.565	9.622	34.976	3.539

blood flow and its stability for individual groups. A higher flow is correlated with a higher scattering against the average data set. Obese individuals without diabetes have, in any case, a higher cerebral blood flow than obese individuals with diabetes. The control group is approximately in the middle of the range. This leads to the conclusion that a body weight above optimum is correlated with an increase in blood flow. The above-average increase in heart rate in obese individuals may be explained, which leads to its significant burden and correlated diseases and was confirmed in other studies [6]. The situation is reversed in people with diabetes. The collected data do not allow to determine this relation for diabetics with normal body weight; however, the blood flow for the subjects described in this study decreases. This may be explained by the decrease in blood vessel cross-section, which was proven in the study [22].

The REX Toolkit, part of the large Toolkit (CONN) [25] was used for ROI-based analysis. The mean values CBF for the regions from the AAL and Brodman atlases were determined on the basis of the whole brain (CBF) and gray matter (CBF-GM) images. Statistically significant results were determined by comparing the Student's t-test result with the limits, depending on the degree of freedom of the data system considered and the confidence level, set at 95%. (Table 2-6)

Two-sample t-test analysis was used for whole brain analysis of differences between all groups. Due to the small size of the groups, the obtained

Fig. 8.   The result of analysis two-sample t-test between O-NT2D and O-T2D for a confidence level of 0.001.

results should be treated as pilot tests. The analysis of results between obese without diabetes O-NT2D and obese with diabetes O-T2D, for a significance level of 0.001 showed differences in cerebral flow inside the brain mask. The obtained results are presented in Figure 8.

DISCUSSION

The aim of the present study was to analyse statistical data from three groups of subjects and to search for possible differences in cerebral blood flow between these groups: control, obese without diabetes and obese with diabetes. The study was also focused on the principle of the method of arterial blood spine marking and the SPM12 toolbox, which is used to analyze imaging data from MRI. Using the Matlab environment, the Processing_step script was written to automatically process the data using the SPM12 toolbox functions: DICOM import, correction, segmentation, normalization, multiplication and smoothing of images. Then, using the previously prepared data, a statistical analysis of the data was carried out, using a proprietary ttest script, written in the Matlab environment, and two functions of the SPM12 toolbox. The obtained results were analysed and conclusions were drawn. Statistical analysis of the data using the ttest function gave results showing the differences in cerebral blood flow between the analysed groups.

In the preliminary analysis, we have observed reduced CBF only in the morbidly obese group with comorbid T2D, as compared to both controls and a decade younger group of morbidly obese patients without T2D. This finding is consistent with literature [20]. The age differences between the morbidly obese groups simply reflects the fact that T2D develops as a co-morbid condition of obesity. Therefore, we are unable to discern whether the CBF deficits are simply due to the existence of comorbid T2D, or they developed as an interplay between (morbid) obesity, aging and T2D.

The author's scripts developed for the purpose of this work were constructed in a way that allows for the preparation and analysis of any number of subjects and groups. Thus, this tool can be used to analyze a larger number of subjects in the future, in the next edition of the research program, for which an application to the National Science Centre is prepared.
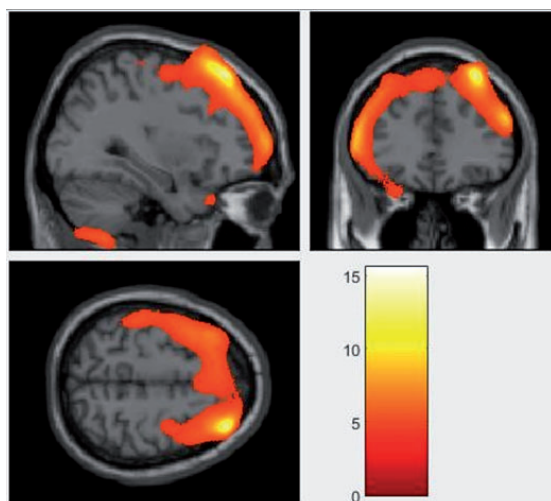
CONCLUSIONS

A pipeline to numerically process ASL-CBF data was created and used to analyse the small dataset. The analyses indicated that not morbid obesity per se, but morbid obesity combined with co-morbid type 2 diabetes is associated with widespread reductions in cerebral perfusion. The results are in line with other studies that were limited to subjects with lower stages of overweight and obesity. Furthermore, the methodology may be applied to study changes in brain perfusion evoked by simulated hypergravity with Lower-Body Negative Pressure (LBNP) device placed within a magnetic resonance scanner or perfusion changes induced by hypoxia.

ACKNOWLEDGEMENTS

AUTHORS' DECLARATION:

REFERENCES

1. [Anonym]. User manual mr750w 3.0t – 3dasl concept. In: Company GE ed; 2013.

2. Aghjayan SL, Stillman CM, El Nokali NE et al. Differences in adolescent cerebral perfusion as a function of obesity: Results from the flex-brain study. Obesity 2021; 29: 1171-1177.

3. Alsop DC, Detre JA, Golay X et al. Recommended implementation of arterial spin-labeled perfusion mri for clinical applications: A consensus of the ismrm perfusion study group and the european consortium for asl in dementia. Magn Reson Med 2015; 73: 102-116.

4. Amen DG, Wu J, George N et al. Patterns of regional cerebral blood flow as a function of obesity in adults. Journal of Alzheimers Disease 2020; 77: 1331-1337.

5. Carmack PS, Spence J, Gunst RF et al. Improved agreement between talairach and mni coordinate spaces in deep brain regions. Neuroimage 2004; 22: 367-371.

6. Czech A, Bernas M, Tatoń J. Cardiovascular symptoms of overweight and obesity. Endocrinology, Obesity, and Metabolic Disorders 2007; 2: 85-94.

7. Gauvrit J-Y, Jean-Christophe F. Asl - arterial spin labelling. First Italian-French Updae Imaging (IPUM); March 23-24, 2018.2018; Milan.

8. Gaździńska AP, Mojkowska A, Janewicz M et al. Real life changes in physical activity due to intragastric balloon therapy and their relationship to improving cognitive functions: Preliminary findings. Obes Surg 2020; 30: 2821-2825.

9. Gaździńska AP, Mojkowska A, Zielinski P et al. Changes in resting metabolic rate and body composition due to intragastric balloon therapy. Surg Obes Relat Dis 2020; 16: 34-39.

10. Gaździński S, Kornak J, Weiner MW et al. Body mass index and magnetic resonance markers of brain integrity in adults. Ann Neurol 2008; 63: 652-657.

11. Gaździński S, Millin R, Kaiser LG et al. Bmi and neuronal integrity in healthy, cognitively normal elderly: A proton magnetic resonance spectroscopy study. Obesity 2010; 18: 743-748

12. Gaździński SP, Gazdzinska AP, Orzel J et al. Intragastric balloon therapy leads to normalization of brain magnetic resonance spectroscopic markers of diabetes in morbidly obese patients. NMR Biomed 2018; 31.

13. Gaździńska A, Wójcik R, Janewicz M et al. Excess body weight as a risk factor to wellbeing and performance of flight personnel: Potential strategies of prevention. Polish Journal of Aviation Medicine 2014; 20: 27-36.

14. Janewicz M, Binder M, Gaździńska A et al. Cognitive improvements following body mass reduction induced by intragastric balloon in morbidly obese patients. A preliminary study. The Polish Journal of Aviation Medicine, Bioengineering and Psychology 2018; 24: 5-11.

15. Josephs O, Turner R, Friston K. Event-related fmri. Hum Brain Mapp 1997; 5: 243-248.

16. Kepes Z, Nagy F, Budai A et al. Age, bmi and diabetes as independent predictors of brain hypoperfusion. Nuclear Medicine Review 2021; 24: 11-15.

17. Knight SP, Laird E, Williamson W et al. Obesity is associated with reduced cerebral blood flow - modified by physical activity. Neurobiol Aging 2021; 105: 35-47.

18. Mutsaerts H, Steketee RME, Heijtel DFR et al. Inter-vendor reproducibility of pseudo-continuous arterial spin labeling at 3 tesla. PLoS One 2014; 9.

19. Peng SL, Chen CM. The influence of obesity on cerebral blood flow in young adults using arterial spin labeling mri. NMR Biomed 2020; 33.

20. Redel JM, DiFrancesco M, Lee GR et al. Cerebral blood flow is lower in youth with type 2 diabetes compared to obese controls: A pilot study. Pediatr Diabetes, DOI: 10.1111/pedi.13313.

21. Sahin I, Alkan A, Keskin L et al. Evaluation of in vivo cerebral metabolism on proton magnetic resonance spectroscopy in patients with impaired glucose tolerance and type 2 diabetes mellitus. J Diabetes Complications 2008; 22: 254-260.

22. Snarska KK, Bachorzewska-Gajewska H, Kapica-Topczewska K et al. Hyperglycemia and diabetes have different impacts on outcome of ischemic and hemorrhagic stroke. Arch Med Sci 2017; 13: 100-108.

23. Tzourio-Mazoyer N, Landeau B, Papathanassiou D et al. Automated anatomical labeling of activations in spm using a macroscopic anatomical parcellation of the mni mri single-subject brain. Neuroimage 2002; 15: 273-289.

24. Volkow ND, Wang GJ, Telang F et al. Inverse association between bmi and prefrontal metabolic activity in healthy adults. Obesity 2009; 17: 60-65.

25. Whitfield-Gabrieli S, Nieto-Castanon A. Conn: A functional connectivity toolbox for correlated and anticorrelated brain networks. Brain Connectivity 2012; 2: 125-141.

26. Willette AA, Kapogiannis D. Does the brain shrink as the waist expands? Ageing Research Reviews 2015; 20: 86-97.

27. Willeumier KC TD, Amen DG. Elevated bmi is associated with decreased blood flow in the prefrontal cortex using spect imaging in healthy adults. Obesity 2011; 19: 1095-1097.

28. Williams DS, Detre JA, Leigh JS et al. Magnetic-resonance-imaging of perfusion using spin inversion of arterial water. Proc Natl Acad Sci U S A 1992; 89: 212-216.